The EMBO Journal vol.14 no.20 pp.5006–5015, 1995

A single amino acid in the SH3 domain of Hck determines its high affinity and specificity in binding to HIV-1 Nef protein

Chi-Hon Lee[1], Benjamin Leung[2], Mark A.Lemmon[3], Jie Zheng[4], David Cowburn[4], John Kuriyan[1,5] and Kalle Saksela[2,6]

[1]Laboratory of Molecular Biophysics, [2]Laboratory of Molecular Cell Biology, [4]Laboratory of Physical Biochemistry, [5]Howard Hughes Medical Institute, The Rockefeller University, 1230 York Avenue, New York, NY 10021 and [3]Department of Pharmacology, New York University Medical Center, New York, NY 10016, USA

[6]Corresponding author

We have examined the differential binding of Hck and Fyn to HIV-1 Nef to elucidate the structural basis of SH3 binding affinity and specificity. Full-length Nef bound to Hck SH3 with the highest affinity reported for an SH3-mediated interaction (K_D 250 nM). In contrast to Hck, affinity of the highly homologous Fyn SH3 for Nef was too weak (K_D >20 μM) to be accurately determined. We show that this distinct specificity lies in a variable loop, the 'RT loop', positioned close to conserved SH3 residues implicated in the binding of proline-rich (PxxP) motifs. A mutant Fyn SH3 with a single amino acid substitution (R96I) in its RT loop had an affinity (K_D 380 nM) for Nef comparable with that of Hck SH3. Based on additional mutagenesis studies we propose that the selective recognition of Nef by Hck SH3 is determined by hydrophobic interactions involving an isoleucine residue in its RT loop. Although Nef contains a PxxP motif which is necessary for the interaction with Hck SH3, high affinity binding was only observed for intact Nef protein. The binding of a peptide containing the Nef PxxP motif showed >300-fold weaker affinity for Hck SH3 than full-length Nef.
Keywords: HIV/PxxP motif/SIV/tyrosine kinase

Introduction

Src homology 3 (SH3) domains are found in many different proteins involved in intracellular signaling and cytoskeletal organization (Mayer and Baltimore, 1993; Pawson and Schlessinger, 1993; Musacchio *et al.*, 1994b; Schlessinger, 1994; Cohen *et al.*, 1995). Characterization of cellular proteins that bind to them has led to the identification of short proline-rich protein sequences as ligands for SH3 domains (Cicchetti *et al.*, 1992; Ren *et al.*, 1993; Musacchio *et al.*, 1994b; Cohen *et al.*, 1995). Selection of additional SH3 binding sites from peptide libraries has further established a minimal PxxP consensus as a critical determinant for SH3 binding (Rickles *et al.*, 1994; Yu *et al.*, 1994).

The three-dimensional structures of many different SH3 domains have been determined by NMR spectroscopy or X-ray crystallography (Kuriyan and Cowburn, 1993; Musacchio *et al.*, 1994b), including complexes of the SH3 domains of Src (Feng *et al.*, 1994), PI3K (Yu *et al.*, 1994), Sem5/Grb2 (Lim *et al.*, 1994; Terasawa *et al.*, 1994; Wittekind *et al.*, 1994), Abl, Fyn (Musacchio *et al.*, 1994a) and Crk (Wu *et al.*, 1995) with short peptides containing PxxP motifs. Despite the variability in their primary structures, these SH3 domains share a very similar overall structure and mode of binding to PxxP peptides. The SH3 target peptides adopt a left-handed polyproline II helix (PPII) conformation in which the critical proline residues are on two edges of the helix and face the relatively flat binding surface formed by conserved hydrophobic residues in the SH3 domain. Part of the binding affinity is contributed by hydrophobic interactions between residues of the SH3 domain and the PxxP defining prolines, as well as other residues in the peptide. In addition, most SH3–PxxP interactions involve ionic interactions between a basic residue positioned before or after the PxxP motif and a highly conserved acidic residue in the SH3 domain (D99 in Src; g in Figure 4B). Interestingly, the position of this basic residue relative to the PxxP motif appears to determine the orientation ('plus' or 'minus') of the pseudo-symmetric PxxP-containing peptide on the SH3 surface (Feng *et al.*, 1994; Lim *et al.*, 1994) (see Figure 4A).

An important function of SH3 domains is to participate in highly selective protein–protein interactions. Therefore, it seems paradoxical that PxxP SH3 binding generally appears to be of low affinity and specificity. Some degree of specificity in peptide recognition has been described, however. Abl SH3 does not bind well to ligands of the Src family SH3s and vice versa (Cheng *et al.*, 1994; Rickles *et al.*, 1994; Yu *et al.*, 1994; Alexandropoulos *et al.*, 1995). This appears to be due to the lack of an acidic residue in Abl SH3 (equivalent to Src D99) that is found in Src family SH3s, as well as in most other SH3 domains. Furthermore, binding of a peptide from the guanine nucleotide exchange factor C3G to the N-terminal SH3 domain of Crk is relatively specific (Knudsen *et al.*, 1994, 1995). This interaction was shown to involve a lysine residue in the C3G peptide that is coordinated by three negatively charged side chains in a highly acidic loop of Crk SH3 (Wu *et al.*, 1995), known as the RT loop because of functionally important arginine and threonine residues in the Src SH3 domain (Kato *et al.*, 1986; Potts *et al.*, 1988). Nevertheless, an additional level of complexity giving rise to more specificity for SH3-mediated protein–protein interactions is anticipated to exist.

It has recently been found that the human immunodeficiency virus type 1 (HIV-1) Nef protein binds to the SH3 domains of a subset of Src family kinases in a distinctly specific manner (Saksela *et al.*, 1995). Nef contains a PxxP motif which can mediate binding to the SH3 domains of Hck and Lyn, but not to those of other

tested Src family kinases, such as Fyn, or less related SH3 domains. The SH3 binding capacity of Nef is necessary for optimal spread of HIV-1 infection in primary cell cultures, suggesting that the virus has evolved to exploit SH3-mediated cellular processes to enhance its replication. Molecular characterization of the interaction between HIV-1 Nef and Hck SH3 could therefore not only elucidate the structural basis of SH3 binding specificity, but may also be helpful for development of novel therapeutic strategies aimed at inhibition of HIV-1 replication.

In this study we have used quantitative assays to examine the structural determinants of the differential affinity of Hck and Fyn SH3 domains for Nef. We show that the high affinity of binding of Hck SH3 to Nef can be transferred to Fyn by a single Arg→Ile substitution in the RT loop. Furthermore, we show that the high affinity, as well as the distinct specificity, of the Nef–Hck interaction is evident only when the Nef PxxP motif is present within the intact Nef protein. These studies indicate that regions of intact SH3 binding proteins outside the linear sequence containing the PxxP motif can play a critical role in determining affinity and specificity.

Results

High affinity binding of Nef to Hck SH3

To study the structural basis of the affinity and selectivity of the interaction between HIV-1 Nef protein and the Hck SH3 domain we have used surface plasmon resonance (SPR) measurements and isothermal titration calorimetry (ITC) (Wiseman *et al.*, 1989; O'Shannessy *et al.*, 1993; Ladbury *et al.*, 1995) to examine binding of wild-type and mutant Nef proteins to various SH3 domains. These SH3 domains were expressed as glutathione S-transferase (GST) fusion proteins, biotinylated and immobilized onto streptavidin-coated chips of a BIAcore biosensor apparatus. The full-length wild-type Nef protein produced for these experiments corresponds to the HIV-1 NL4-3 Nef, but has a Thr→Arg mutation at position 71 in order to mimic the amino acid sequence that occurs in this region of most Nef alleles that have been obtained directly from patients (Shugars *et al.*, 1993; Huang *et al.*, 1995). Arg71 is adjacent to amino acid residues of Nef that are involved in SH3 binding and may influence this interaction (Saksela *et al.*, 1995). As a negative control we also produced and tested a mutant HIV-1 NL4-3-derived Nef protein (Nef-PA1) which carries a double Pro→Ala substitution that disrupts the two internal prolines of the conserved Nef tetraproline repeat. Nef-PA1 is unable to bind to Hck SH3 (Saksela *et al.*, 1995).

Figure 1A shows SPR profiles obtained after flowing buffer containing various concentrations of Nef over a biosensor chip coated with Hck SH3. Corresponding SPR signals obtained in parallel by testing identical concentrations of Nef on biosensor chips without SH3 proteins (to control for bulk refractive index effects) have been subtracted from these values. Therefore, these profiles, as well as those shown later, reflect specific association between Nef and the immobilized SH3 protein. Based on these measurements, the equilibrium dissociation constant (K_D) for the interaction between Nef and Hck SH3 was determined by Scatchard analysis of the SPR response at equilibrium (Figure 1B) and was found to be

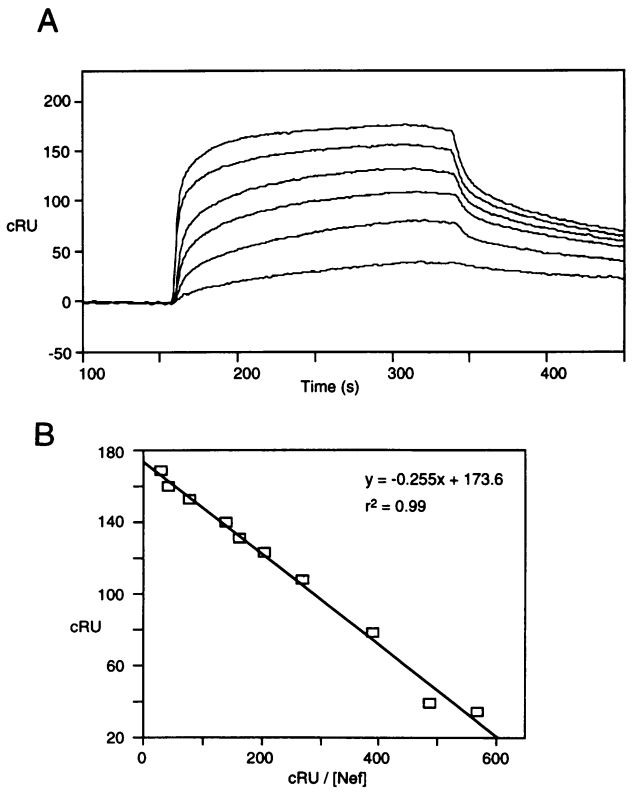

Fig. 1. Determination of the equilibrium dissociation constant for the Nef–Hck SH3 interaction using surface plasmon resonance (SPR). (**A**) The response functions (sensorgrams) shown illustrate specific binding and dissociation profiles obtained after Nef protein at various concentrations was added to the buffer flowing over a biosensor chip coated with GST–Hck SH3. The data in these sensorgrams and (**B**) in the Scatchard analysis are expressed as corrected response units (cRU), as the contribution by the bulk refractive index (background) has been subtracted. For clarity only the sensorgrams obtained using 0.08, 0.2, 0.4, 0.8, 2 and 6 μM Nef are shown in (A), whereas the SPR response values from all 10 concentrations of Nef tested (ranging from 0.06 to 6 μM) were included in the Scatchard analysis in (B). The data is best fitted by a line with equation $y = -0.255x + 173.6$, the coefficient of determination (r^2) being 0.99.

250 nM. The linearity of the Scatchard plot over a wide range of tested Nef concentrations (0.06–6 μM) indicates that Nef–Hck SH3 binding represents a simple bimolecular interaction. As seen in Figure 1A, the on-rate for Nef binding to Hck SH3 was very rapid. Due to this rapid on-rate, significant re-binding of dissociated Nef probably also occurred under these conditions. Therefore, it was not possible to reliably measure off- or on-rates, since both would be artificially influenced by experimental variables of the system, such as the flow rate, concentration of Nef and the surface density of Hck SH3. In contrast, the Scatchard analysis used to determine the K_D values is not sensitive to these effects, since it relies only on the SPR response at equilibrium.

The low K_D value determined for binding of Nef to Hck SH3 (250 nM) indicates an affinity that is significantly greater than previously reported for any other SH3–PxxP interaction (K_D 1–50 μM). To confirm this unusually high affinity using another independent methodology we examined the Hck–Nef interaction by ITC (Wiseman *et al.*, 1989; Lemmon and Ladbury, 1994). In ITC experiments we used free Hck SH3, rather than the GST–Hck SH3

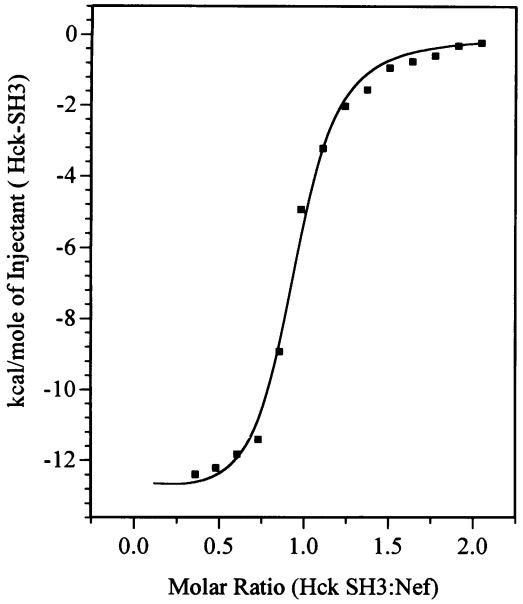

Fig. 2. Characterization of Nef binding to the Hck SH3 domain using ITC. The titration consisted of 16 injections of 15 µl Hck SH3 domain into Nef protein solution. The points correspond to the enthalpy per mole of injectant per injection. The first two data points were removed because of a noisy baseline. The remaining data points were fitted by a non-linear least squares algorithm, giving a K_B of 53.3 ± 9.3×10^{-5}/M (corresponding to a K_D of 188 ± 34 nM), a ΔH of −12.75 ± 0.32 kcal/mol and a stoichiometry (N) of 0.893 ± 0.013.

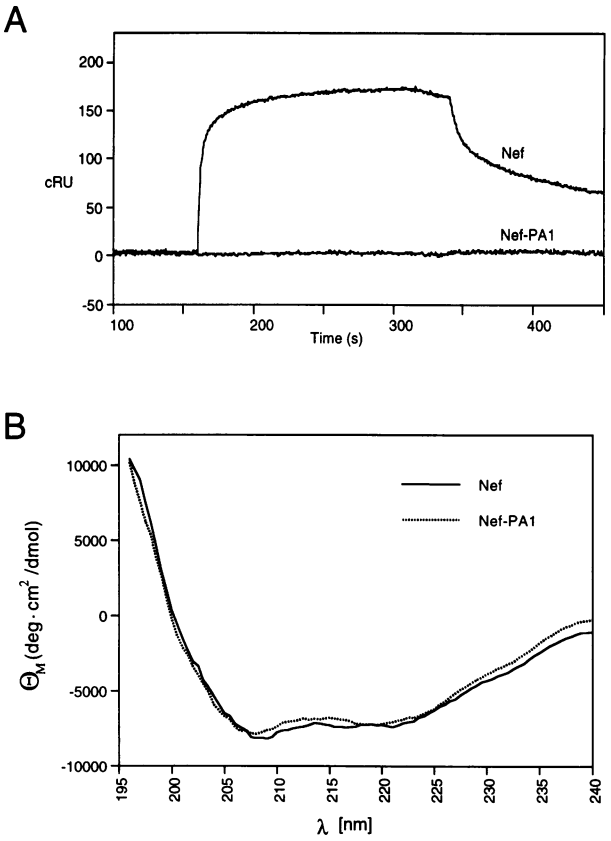

Fig. 3. (**A**) Comparison of binding of wild-type Nef and the PxxP-defective mutant Nef-PA1 to Hck SH3. SPR profiles using Nef (upper line) at a concentration close to saturation (8 µM) and Nef-PA1 (lower line) at the same concentration are shown. Both sensorgrams were derived and corrected for the bulk refractive index effect as in Figure 1A. (**B**) CD spectra of Nef (solid line) and Nef-PA1 (dashed line). Spectra of Nef and Nef-PA1 were recorded at 15°C using a 50 µM protein concentration in the same buffer as in the SPR experiments shown in (A). Five individual measurements were averaged and expressed as molar mean residue ellipticity (Θ_M) values.

fusion protein, while the other ITC experimental conditions, including buffer composition and temperature, were essentially identical to those used in the SPR studies. The heat released upon each of the 16 sequential injections of Hck SH3 into a Nef solution was integrated and normalized per mole of injectant. As shown in Figure 2, a plot of heat released per mole of Hck SH3 injected against the SH3:Nef molar ratio takes the form of a sigmoid titration curve, with its midpoint occuring at a ratio of 1:1. The data were fitted to the curve shown using a non-linear least squares algorithm (Wiseman *et al.*, 1989) and the enthalpy per mole of ligand added (ΔH), the association constant K_B (= 1/ K_D) and stoichiometry were derived. The K_D value (188 ± 34 nM) obtained using ITC is comparable with that observed by SPR and the stoichiometry for this interaction (1:0.89) was found to be very close to a ratio of 1:1. The ΔH for this interaction at 25°C was −12.75 kcal/mol, which together with the experimentally derived K_B value, gives an entropy change ΔS^o = −12.0 cal/K/mol. The large negative enthalpy change and the small unfavorable entropy change observed for the Nef–Hck SH3 interaction indicate that under the experimental conditions used this interaction is mainly driven by exothermic enthalpy.

In direct contrast to Nef, no binding to Hck SH3 was observed when the mutant Nef-PA1 protein was tested using SPR (Figure 3A), indicating that the high affinity of the Nef–Hck SH3 interaction is critically dependent on an intact Nef PxxP motif. To confirm that this lack of binding was due to the defective PxxP motif of Nef-PA1, rather than a non-specific structural alteration in the protein caused by the introduced Pro→Ala changes we compared the wild-type Nef and Nef-PA1 proteins by circular dichroism (CD) spectroscopy. As seen in Figure 3B, under experimental conditions similar to those used for the SPR measurements, the CD spectra of Nef and Nef-PA1 were virtually identical, excluding the possibility of gross structural abnormalities in Nef-PA1. It should be noted that Nef proteins used in all these experiments were highly purified and free of GST. The lack of apparent structural alterations in Nef-PA1 by CD is in agreement with our previous observations, which indicate that despite loss of SH3 binding and hence the ability to increase HIV replication, Nef-PA1 can still mediate down-modulation of surface expression of the CD4 molecule (Saksela *et al.*, 1995). Moreover, the CD spectra obtained for these Nef proteins appear identical to those published by Wittinghofer and colleagues in their biochemical characterization of the HIV-1 NL4-3 Nef protein (Wolber *et al.*, 1992).

In summary, these data show that native Nef protein can bind in solution to the Hck SH3 domain with very high affinity and that this binding is absolutely dependent on a functional Nef PxxP site.

Sequence comparison and molecular modeling

In an effort to understand the structural basis of specific SH3 binding by Nef we have aligned the PxxP motif of

Nef with other PxxP motifs (Figure 4A), as well as the sequence of Hck SH3 with those of other SH3 domains (Figure 4B). To illustrate the potential interactions between the Nef PxxP peptide and the Hck SH3 domain we have modeled the complex on the basis of known SH3 peptide structures (Figure 4C). Figure 4A shows an alignment of various SH3 binding ligands adapted from Lim *et al.* (1994). Based on the molecular modeling, as well as on experimental data, we suggest that the two middle prolines of the HIV-1 Nef tetraproline repeat constitute the PxxP defining residues and that the positioning of the HIV-1 Nef residue Arg77, which is very well conserved among different primate immunodeficiency viruses, defines binding of the Nef PxxP peptide in the 'minus' orientation. This arginine residue, in the P_{-3} binding pocket, would thus be involved in interactions with acidic residues in the RT loop of Hck SH3 (residues f and g in Figure 4B and C). The critical role of the two internal prolines (PVRPQVPLRP) is supported by data from filter binding experiments indicating that mutation of either one of them alone (PVRAQVPLRP or PVRPQVALRP) abolishes binding to Hck SH3 and that a peptide overlapping the corresponding region in SIVmac239 Nef (LVGISVRPKV-PLRTMSYK) can bind to Hck SH3, despite its lack of both of the external prolines (data not shown). Moreover, a hydrophobic residue (Val74) assigned to binding pocket P_0 is also extremely well conserved among Nef proteins encoded by different viruses (including SIVmac239). Thus this valine and the arginine in the P_{-3} pocket form the two asymmetric interactions defining the 'minus' orientation (Feng *et al.*, 1994; Lim *et al.*, 1994).

The structural model (Figure 4C) described here was generated in a simplistic manner and relies on the strong conservation of three-dimensional structure in SH3 domains (Wu *et al.*, 1995). In particular, the model is based on the structures of the highly homologous Fyn and Lck SH3 domains, as well as the Crk-SH3–peptide complex (Noble *et al.*, 1993; Eck *et al.*, 1994; Wu *et al.*, 1995). We modeled the other arginine residue in this region of Nef (Arg71) in position P_3, so that the aliphatic region of the side chain packs against the face of two conserved tyrosines residues, Tyr66 and Tyr111 (a and l), of the Hck SH3 domain. The guanido group of Arg71 may hydrogen bond with Asp67 (b) and Glu69 (d). Unlike the laboratory-adapted strain HIV-1 NL4-3, almost all Nef genes isolated from patients encode an arginine or a lysine at position 71 (Shugars *et al.*, 1993; Huang *et al.*, 1995) and an arginine residue in this position of Nef (as compared to Thr) increases its binding to Hck SH3 (Saksela *et al.*, 1995).

The RT loop determines the differential affinity of Hck and Fyn SH3 domains

The SH3 domains of Hck and Lyn can bind to Nef, whereas the highly homologous SH3 domains of Fyn or Lck do not (Saksela *et al.*, 1995). Based on our modeling of the Hck SH3–Nef interaction (Figure 4A and C) and the alignment of the amino acid sequences of various SH3 domains (Figure 4B), our attention was drawn towards adjacent isoleucine (e in Figure 4B) and histidine residues that are present in the SH3 RT loops of Hck and Lyn, but not in other SH3 domains. To test the importance of this part of the RT loop in differential binding to Nef PxxP we made a reciprocal change involving the three divergent amino acids in this region of Hck and Fyn SH3s. This resulted in a mutant Hck SH3 domain which has a Fyn-like RT loop (Hck-RTE) and a mutant Fyn SH3 which has a Hck-like RT loop (Fyn-IHH) (see Table I).

The affinity of these mutant SH3 domains in binding to Nef was then compared with wild-type Hck and Fyn SH3 domains by SPR. As expected, in contrast to the strong interaction between Nef and Hck SH3, binding of Nef to Fyn SH3 was very weak (Figure 5). Although some binding over the background was observed using high concentrations of Nef (8 μM), these sensorgrams were not sufficiently well defined to accurately determine a K_D value for this interaction (estimated to be weaker than K_D 20 μM) by Scatchard analysis. In contrast, when the Fyn SH3 domain with a Hck-like RT loop (Fyn-IHH) was tested, good binding to Nef (K_D 2.0 μM) was observed (Table I). Conversely, substituting the RT loop of Hck SH3 with that of Fyn (Hck-RTE) resulted in loss of quantifiable binding to Nef (K_D >20 μM).

We then constructed and tested additional mutant Fyn SH3 domains to examine the individual contribution of each of the three Hck-specific amino acids (IHH) in providing Nef binding affinity for Fyn SH3 (see Table I). We found that the affinity of Fyn-IH was similar (K_D 3.1 μM) to that of Fyn-IHH (K_D 2.0 μM), suggesting that the second histidine residue in Fyn-IHH did not contribute to its increased affinity for Nef. Like wild-type Fyn SH3, binding of Nef to Fyn-H was too weak to be accurately quantitated by the current assay (K_D >20 μM), indicating that the first histidine in the Hck-like RT loop of Fyn-IHH does not increase binding to Nef when introduced alone into Fyn SH3. In contrast, Fyn-I bound to Nef even better than Fyn-IHH (or Fyn-IH), showing an affinity for Nef (K_D 380 nM) almost as great as that of Hck SH3 (K_D 250 nM). This suggests that the increased affinity of Fyn-IHH for Nef resulted primarily from replacement of the Fyn residue Arg96 by an isoleucine (position c in Figure 4B). The fact that Fyn-I binds Nef more strongly than Fyn-IH or Fyn-IHH seems counterintuitive, given that both Hck and Lyn have a histidine residue following this isoleucine. The reason for this is unclear in the absence of a structure of the mutant Fyn SH3 domain. One possibility is that in Fyn-IH and Fyn-IHH the presence of this histidine may interfere with interaction between the arginine residue of the Nef PxxP motif and Asp100 in Fyn.

To explore the basis for the increased affinity of the mutant Fyn SH3 domain (Fyn-I) for Nef we replaced the naturally occurring arginine residue (Arg96) in this position of Fyn with other amino acids (Table I). These substitutions included a basic residue (lysine, Fyn-K), an acidic residue (aspartic acid, Fyn-D) and a non-polar residue with reduced hydrophobic surface (alanine, Fyn-A). None of these Fyn SH3 mutants bound to Nef as strongly as Fyn-I. However, in contrast to Fyn-K and Fyn-D, which did not bind to Nef any better than wild-type Fyn SH3, Fyn-A showed a relatively high affinity for Nef (K_D 4.4 μM). The fact that lysine and aspartate substitutions at this position lead to equally poor binding indicates that repulsion by the positive charge of the Fyn residue Arg96 (e in Figure 4B) is not the major determinant of the low affinity of Fyn. Rather, the interaction involves

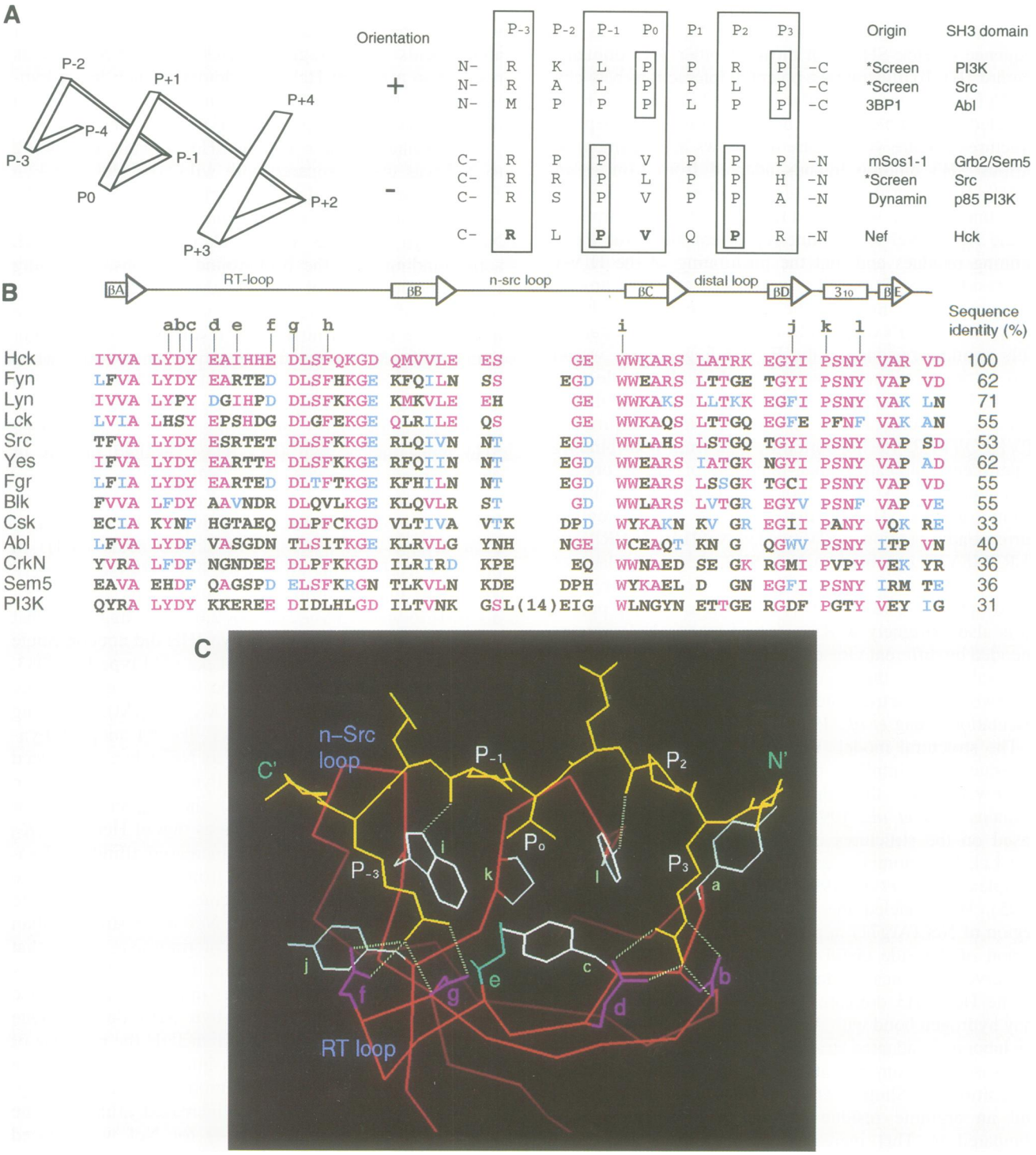

Fig. 4. (**A**) Alignment of the Nef PxxP motif (RPQVPLR, amino acids 71–77 in HIV-1 NL4-3 Nef) with other peptides binding to different SH3 domains in 'plus' or 'minus' orientations according to Lim *et al.* (1994) and Feng *et al.* (1994). The Nef residues which are highly conserved among primate immunodeficiency viruses are indicated in bold type. The positions P_{-3}, P_{-1}, P_0, P_2 and P_3 contain the ligand residues which interact with the conserved hydrophobic residues forming the binding interface of SH3 domains. The spacing of positions are also shown in the ribbon diagram representing a left-handed PPII helix. (**B**) Alignment of SH3 domain amino acid sequences. The indicated secondary structure is based on the crystal structure of the Fyn SH3 domain (Noble *et al.*, 1993). The five antiparallel β-sheets (A–E) forming the SH3 structure, as well the loops between them, are indicated. The amino acid identity to Hck in this region is indicated as a percentage and by purple coloring in the alignment. Amino acid similarity (D/E, K/R, S/T, W/F/Y and A/L/I/V were considered similar) is indicated by light blue coloring. The conserved acidic (b, d, f and g) and hydrophobic (a, c, h, i, j, k and l) residues implicated in ligand binding are indicated on top of the amino acid alignment. (**C**) Hypothetical model of potential interactions between Hck SH3 and the Nef PxxP motif. The C^{α} backbone of Hck SH3 is shown in red and the Nef PxxP motif (sequence VRPQVPLRP, modeled in the 'minus' orientation, right to left) is shown in yellow. The conserved hydrophobic residues (a, c, h, i, j, k and l) forming the binding surface of the Hck SH3 domain are shown in white, except for residue Phe77 (h), which is omitted for clarity. The acidic residues (f and g) in the RT loop which are shown to interact with the arginine residue at the P_{-3} position of the Nef PxxP motif and the acidic residues (b and d) which are modeled to interact with the arginine residue at the P_3 position are shown in purple. The isoleucine residue (e) in the RT loop which is implicated in the interaction with Nef is shown in blue. This model is based on SH3–peptide complexes of known structure (Noble *et al.*, 1993; Eck *et al.*, 1994; Wu *et al.*, 1995).

Table I. Summary of the quantitative Nef–SH3 binding data

	RT-loop	Nef protein	Nef peptide PVRPQVPLRPMT
		K_D (μM)	K_D (μM)
Hct-wt	...YDY EAIHHE DLS...	0.25 ± 0.05	91 ± 5
Hck-RTE	...YDY EARTEE DLS...	>20	N.D.
Fyn-wt	...YDY EARTED DLS...	>20	202 ± 7
Fyn-IHH	...YDY EAIHHD DLS...	2.0 ± 0.5	N.D.
Fyn-IH	...YDY EAIHED DLS...	3.1 ± 0.2	N.D.
Fyn-H	...YDY EARHED DLS...	>20	N.D.
Fyn-I	...YDY EAITED DLS...	0.38 ± 0.04	91 ± 4
Fyn-A	...YDY EAATED DLS...	4.4 ± 0.8	N.D.
Fyn-D	...YDY EADTED DLS...	>20	N.D.
Fyn-K	...YDY EAKTED DLS...	>20	N.D.

Amino acid sequences in the region of the SH3 domain RT loop that were targeted for mutagenesis analysis are shown for wild-type (wt) Hck and Fyn and the derived altered SH3 proteins. The introduced amino acid changes are underlined. The equilibrium dissociation constants (K_D) for binding of these SH3 domains to Nef protein or a 12mer peptide overlapping the Nef PxxP motif (PVRPQVPLRPMT), measured based on surface plasmon resonance or tryptophan fluorescence respectively, are shown on their right.

specific selection of Hck because of the isoleucine side chain at this position.

Nef PxxP peptide alone has low affinity and limited specificity in SH3 binding

The loss of binding to Hck SH3 by the Nef mutant with a double Pro→Ala substitution within its tetraproline repeat region indicated that this PxxP motif is essential for high affinity SH3 binding by Nef. To study the binding properties of an isolated peptide containing the Nef PxxP motif we synthesized a 12mer peptide PVRPQVPLRPMT spanning this region and studied its interaction with different SH3 domains by tryptophan fluorescence (Knudsen *et al.*, 1995). This method is well suited for detection of interactions involving small polypeptides and has the capacity to measure affinities of interactions with K_D values in the high micromolar range.

We found that the affinity of the 12mer Nef peptide in binding to Hck SH3 was 91 μM, indicating that this interaction is >300-fold weaker than that with full-length Nef protein (Table I). Furthermore, we measured a K_D value of 202 μM for the interaction between Fyn SH3 and the Nef peptide, indicating that the differential specificity of Hck SH3, as compared with Fyn SH3, in binding to native Nef protein is much less evident when the Nef PxxP peptide is separated from its natural context.

Nef PxxP motif-mediated SH3 binding examined by a co-precipitation assay

To confirm our results on the specificity and affinity of different SH3 domains in binding to Nef and the Nef PxxP peptide by another technique we developed a robust, semi-quantitative co-precipitation assay (see Materials and methods). As can be seen, increasing amounts of co-precipitating Nef protein was observed using agarose beads coated with the SH3 domains of Hck or Fyn-I, showing apparent saturation between 4 and 16 μg/ml Nef (Figure 6A, panels Hck and Fyn-I). In contrast, no Nef could be co-precipitated using beads coated with Fyn SH3, even when the highest Nef concentration (16 μg/ml) was tested (Figure 6A, right panel). Also in agreement with the BIAcore experiments (Table I), some Nef could be co-precipitated with Fyn-A, but not with Fyn-K or Fyn-D (data not shown).

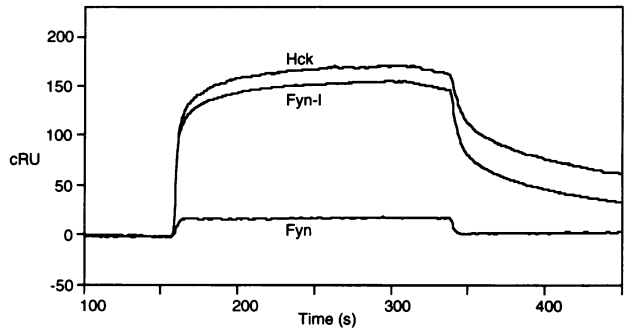

Fig. 5. Differential binding of Nef to Hck, Fyn-I and Fyn SH3 domains. Shown are sensorgrams obtained by testing the binding of 8 μM Nef to wild-type Hck (upper line), Fyn-I (middle line) and wild-type Fyn (lower line) SH3 domains. The amounts of Hck, Fyn-I and Fyn SH3 proteins immobilized on the biosensor chips were similar, corresponding to 430, 400 and 490 RU respectively. All sensorgrams have been corrected for the bulk refractive index effect.

To compare the relative affinities of native Nef protein and the Nef PxxP peptide PVRPQVPLRPMT in binding to the Hck SH3 domain increasing concentrations of this peptide were added into the co-precipitation assay to compete with a constant amount of Nef (4 μg/ml). As seen in Figure 6B, an 800-fold molar excess of the peptide was required to significantly compete with full-length Nef protein in binding to Hck SH3, supporting the magnitude of the differences in their affinities measured by SPR (Nef) and tryptophan fluorescence (Nef PxxP).

As expected, mutant Nef-PA1 protein with a disrupted tetraproline repeat could not be co-precipitated with Hck SH3 (Figure 6C). In contrast, another mutant form of Nef containing a Pro→Ala substitution at position 147 (Nef-A147) bound to Hck SH3 with an apparently similar affinity to the wild-type Nef (Figure 6C), indicating that in the context of native soluble Nef protein the residue Pro147 is not involved in binding to Hck SH3.

Discussion

In this study we show that the basis of the differential affinity of the Hck and Fyn SH3 domains in binding to the HIV-1 Nef PxxP site lies in their RT loops. Both the high affinity and the high selectivity of the Nef–Hck SH3

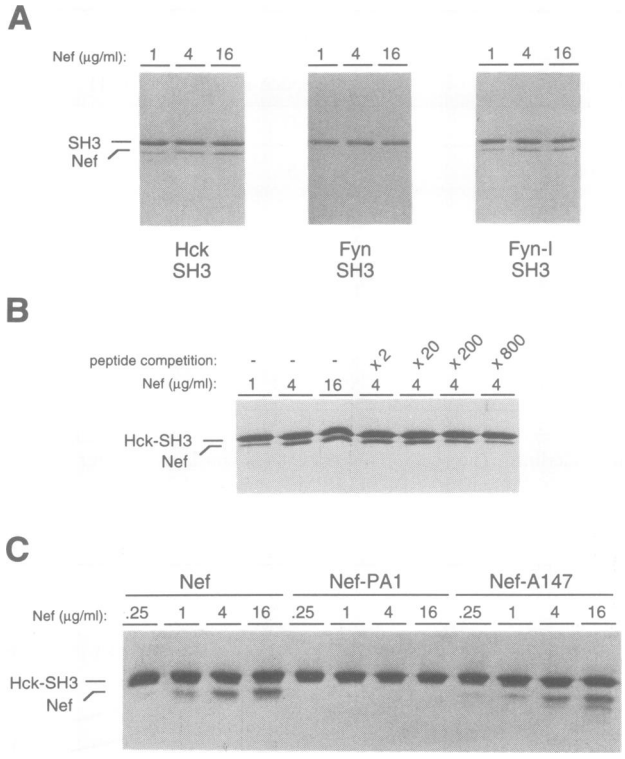

Fig. 6. SH3–Nef co-precipitation assay. (**A**) One microgram of the bead-immobilized GST fusion proteins containing Hck, Fyn or Fyn-I SH3 domains were incubated with increasing concentrations of Nef as indicated. The amount of Nef protein retained with the beads after washes was analyzed by SDS–PAGE. The positions of the GST–SH3 and Nef proteins in the Coomassie Blue stained gels are indicated on the left. (**B**) Beads containing 2 μg GST–Hck SH3 protein were incubated with increasing concentrations of Nef or with 4 μg/ml Nef in the presence of increasing molar excess of the Nef PxxP peptide PVRPQVPLRPMT, as indicated, followed by analysis of co-precipitated Nef protein as in (A). (**C**) Beads containing 4 μg GST–Hck SH3 protein were incubated with increasing concentrations of Nef, Nef-PA1 or Nef-A147, followed by analysis of co-precipitated Nef proteins as in (A). The Nef-A147 protein preparation contained traces of residual free GST protein, which binds to the glutathione beads and can be seen migrating below the Nef protein in these lanes.

interaction were dependent on the presence of the Nef PxxP sequence in the Nef protein, yet were not observed when a 12mer synthetic peptide spanning the Nef tetraproline repeat region was tested. This could be due to at least two reasons: Nef protein might present its Nef PxxP peptide for Hck SH3 in a distinct conformation or additional contacts between Nef and Hck SH3 might contribute to the affinity and specificity of this interaction.

Based on filter binding experiments, it had been suggested that the distally located Nef residue Pro147 might fold to directly participate in Hck SH3 binding (Saksela *et al.*, 1995). However, the present data (Figure 6C) do not support this hypothesis and suggest that mutation of this proline affected binding only through effects on refolding of denatured Nef after transfer to the filter. Nevertheless, our present data support the hypothesis that additional regions of Nef are important for interaction with Hck SH3. Our data indicate that the Hck residue Ile71 (e in Figure 4B) plays a positive role in selection of Nef as a high affinity ligand for its SH3 domain. Since molecular modeling of the Hck SH3–Nef PxxP interaction on the basis of known structures of SH3–peptide complexes does not provide an adequate structural explanation for this observation, we speculate that additional contact(s) provided by the native Nef protein might target this isoleucine residue in the RT loop of Hck SH3.

The weak affinity of Hck SH3 for the synthetic 12mer Nef tetraproline peptide (K_D 91 μM) is in agreement with the K_D values obtained by others using short peptide ligands to measure affinities of SH3–PxxP interactions. Even when optimized sequences have been selected from libraries of synthetic peptides, SH3 binding affinities $>K_D$ 1 μM have not been observed (Yu *et al.*, 1994). Such low values, as well as limited binding specificity, have raised doubts about whether SH3 domains alone can mediate highly selective protein–protein interactions *in vivo*. In fact, most peptides containing a PxxP motif in a hydrophobic background are likely to show some SH3 binding, particularly if a basic residue (b) is present nearby in an appropriate position (bxxPxxP or PxxPxb). Even peptides comprised exclusively of proline bind weakly to SH3 domains and in a <10-fold molar excess can substitute for presumably specific PxxP peptides in competing for binding of cellular proteins to Src family SH3 domains (Weng *et al.*, 1994). It is possible that many of the identified PxxP peptides could mediate much stronger and more selective SH3 binding when present in their native contexts than as free peptides. Conversely, if such an increased affinity is not observed for the full-length protein, not all proteins that contain an SH3 binding peptide may be physiologically involved in interactions with cellular SH3 proteins.

The low selectivity of Hck and Fyn SH3 domains in recognizing the Nef PxxP peptide in solution (91 versus 202 μM) is somewhat surprising in the light of the apparent selectivity that we have previously observed for binding of Hck SH3 (but not Fyn SH3) to fusion proteins containing the Nef PxxP peptide (Saksela *et al.*, 1995). It is possible that the 2-fold difference in their binding affinities may have appeared disproportionately large in the filter binding assay used if the affinity of the weaker interaction (Nef PxxP–Fyn SH3) was below the threshold of efficient detection in this system. In summary, it appears that the presence of the Nef PxxP peptide in the context of whole Nef protein both provides an increased affinity for SH3 binding, as well as influences its specificity.

Guided by the sequence differences between the transforming v-Src and non-transforming c-Src proteins, previous investigations have indicated an important role for the SH3 RT loop in determining the biological properties of the Src protein tyrosine kinase (Kato *et al.*, 1986; Potts *et al.*, 1988). Strikingly, some, but not all, single amino acid changes involving the c-Src residue Arg95 (corresponding to Arg96 in Fyn; e in Figure 4C) resulted in activation of its transforming potential (Potts *et al.*, 1988). While such changes in the RT loop might also result in an altered substrate specificity of the Src kinase, a significant increase in its overall enzymatic activity was observed (Kato *et al.*, 1986; Potts *et al.*, 1988). Recent investigations have provided a possible explanation for this observation, by revealing a role for the SH3 domain in suppression of the intrinsic enzymatic activity of the Src family kinases. This effect has been attributed to the SH3 domain facilitating formation of an intramolecular interaction between the SH2 domain and a phosphotyrosine residue in the

C-termini of Src kinases, resulting in inhibition of catalytic activity (Murphy *et al.*, 1993; Okada *et al.*, 1993; Superti Furga *et al.*, 1993).

A recent mutagenesis analysis by Erpel *et al.* (1995) showed a good correlation between mutations in the Src SH3 domain that resulted in loss of intermolecular ligand recognition and failure to co-operate in its catalytic down-regulation. Interestingly, one Src mutant that had an altered SH3 RT loop was unable to cooperate in Src down-regulation, yet retained its ability to bind to PxxP-containing target proteins. Thus, in the light of our present data and previous published studies, it appears that the RT loop is involved in Src autoregulation, as well as in ligand selection, and the specific structural requirements for these two functions may be different. The gain of function observed in this study upon introducing a single amino acid change into the RT loop of Fyn SH3, such that its affinity towards Nef increased >100-fold, strongly argues that, in contrast to the conserved hydrophobic SH3 residues, the role of the RT loop in ligand binding is not only to provide a scaffold for basic accommodation of the PxxP motif structure, but also to provide selective and high affinity recognition of specific ligands.

In summary, this study defines the specificity and affinity of the Nef–Hck SH3 interaction and the necessity for presentation of the PxxP motif within the context of the intact protein. By examining binding of native Nef protein to the SH3 domain of Hck we demonstrate that SH3–PxxP-mediated protein–protein interactions can have a very high affinity and that in such a case, a small difference in the RT loop region can provide remarkably selective binding properties for two highly homologous SH3 domains. These data seem encouraging for the prospect of interfering with specific SH3–PxxP interactions in the treatment of human disease, specifically, modulating the pathogenesis of HIV infection by blocking the function of Nef.

Materials and methods

Expression vectors and protein purification

Construction of plasmids encoding GST fused to the N-terminus of HIV-1 NL4-3-derived Nef proteins containing various mutations has been described previously (Saksela *et al.*, 1995). Expression and purification of GST–Nef-R71 fusion proteins in *Escherichia coli* strain BL21(DE3) were carried out as suggested by the supplier of the components of the GST fusion protein expression system (Pharmacia). After elution from glutathione–Sepharose beads (Pharmacia) GST–Nef fusion proteins were dialyzed against cleavage buffer (20 mM Tris, pH 8.4, 150 mM KCl, 2.5 mM $CaCl_2$, 20% glycerol) overnight and subjected to thrombin cleavage (6 U thrombin/100 mg fusion protein) for 6 h. This resulted in full-length Nef protein with an additional six amino acids (GSPEFT) at its N-terminus. Cleavage was terminated by adding 1 mM phenylmethylsulfonyl fluoride (PMSF) and 10 mM dithiothreitol (DTT), followed by an overnight dialysis against buffer A (20 mM Tris, pH 7.0, 50 mM KCl, 1 mM PMSF, 10 mM DTT). To separate Nef protein from released GST and from uncleaved fusion protein the dialyzed material was loaded onto a Mono Q HR 10/10 column (Pharmacia) previously equilibrated with buffer B (buffer A with 1 mM DTT) and eluted with a linear NaCl gradient up to 1 M NaCl. Nef protein eluted at 0.1 M NaCl. The fractions containing Nef were pooled and applied to a 20 ml glutathione–Sepharose column to remove residual GST (in buffer B). The flow-through material was collected and precipitated with 80% saturated ammonium sulfate, resuspended in a small volume of buffer B and applied to a Superdex 75 HiLoad gel filtration column pre-equilibrated with buffer B. Nef eluted in a single peak corresponding to the size of a monomer. The fractions containing highly purified Nef protein were concentrated with Centriprep-10 (Amicon) to 30 mg/ml in the same buffer. For each purification 12 l of culture was typically used and the final recovery of purified (>99% purity judged by SDS–PAGE) Nef protein was ~30 mg, as determined spectrophotometrically from their extinction coefficients ε_{280} = 48 790 (experimental value ε_{280} = 44 190; Wolber *et al.*, 1992).

cDNA encoding human Hck (RT-PCR amplified from blood cell RNA from K.Saksela) and Fyn (Kawakami *et al.*, 1986; a kind gift from Avery August and H.Hanafusa, the Rockefeller University) were used as templates to amplify the corresponding SH3 domain regions (Fyn residues 86–143) using primers containing sites for *Eco*RI and *Xho*I restriction endonucleases for cloning into the corresponding sites in pGEX-1ZT [pGEX-1λT (Pharmacia) with a modified polylinker]. The Hck and Fyn SH3 constructs with mutagenized RT loops (Table I) were derived by using a long 5′ PCR primer extending over this region and containing the designed mutations. All SH3 constructs were confirmed by dideoxynucleotide sequencing. GST–SH3 proteins were expressed from these constructs and purified according to the protocol provided with glutathione–Sepharose (Pharmacia) and biotinylated using the ImmunoPure NHS-LC-Biotin reagent as suggested by the supplier (Pierce).

To produce Hck SH3 domain (without GST) for ITC experiments cDNA encoding the SH3 domain of Hck was amplified by PCR using the GST–Hck SH3 construct as template. The amplified DNA fragment was subcloned into an expression vector, pET3a (Novagen), through *Nde*I and *Bam*HI sites. Expression of the Hck SH3 domain using the resulting plasmid was performed according to the protocol provided by the supplier of the pET expression system (Novagen). Protein was purified using standard chromatography techniques, including a DEAE Fast Flow column, a Q-Sepharose Fast Flow column, a Phenyl Sepharose (high performance) column and a Superdex75 HiLoad 16/60 column on an FPLC system (Pharmacia). The protein was concentrated to 10 mg/ml by ultrafiltration (Amicon). For each purification 6 l of culture was typically used and the final recovery of purified (>99% purity judged by SDS–PAGE) Hck SH3 domain was ~12 mg.

Peptide synthesis

Peptide PVRPQVPLRPMT was synthesized by the Biopolymer Synthesis Facility at the Rockefeller University, using conventional technology. The peptide was purified by high performance liquid chromatography and lyophilized prior to resuspension in the buffers used in different experiments. The identity of the peptide was confirmed by mass spectroscopy and its concentration was determined by quantitative amino acid analysis.

Molecular modeling

Crystal structures of the Fyn SH3 (Noble *et al.*, 1993) and Lck SH3-SH2 domains (Eck *et al.*, 1994) and Crk SH3–C3G complex (Wu *et al.*, 1995) were used for modeling Hck–peptide interaction. The Fyn SH3 domain (PDB access number 1shf) shows the highest sequence homology (62% identity) to the Hck SH3 among SH3 domains whose three-dimensional structures have been determined and was therefore used to provide the scaffold of our Hck SH3 model, except for the region of the n-Src loop, in which the sequence of the Lck SH3 domain is more similar to Hck. Three SH3 domain structures were superimposed and residues of Fyn SH3 that are dissimilar to Hck SH3 were changed using program 'O' (Jones *et al.*, 1991). Peptide coordinates were taken from the structure of Crk SH3 complexed with the C3G peptide (Wu *et al.*, 1995) and the residues were changed according to the Nef PxxP motif. X-PLOR (Brünger, 1988) was used to remove unfavorable van der Waals contacts and to improve the geometry by energy minimization and the resulting model was displayed using QUANTA (Molecular Simulations Inc.).

Surface plasmon resonance analysis

Surface plasmon resonance (SPR) experiments were carried out on a BIAcore Biosensor apparatus (Pharmacia Biosensor). Data analysis was performed with the interactive software BIAevalution v2.0 (Pharmacia Biosensor). Biotinylated GST–SH3 proteins were immobilized through biotin–streptavidin interaction onto a Biosensor Chip SA5 (Pharmacia Biosensor) containing pre-immobilized streptavidin. Immobilizations were performed at 25°C with a flow rate of 5 μl/min in HBS running buffer (10 mM HEPES, pH 7.4, 150 mM NaCl, 3.4 mM EDTA, 0.05% Surfactant P20). The amount of biotinylated GST–SH3 fusion protein bound to the chip was monitored by the change in refractive index and controlled to be ~450 RU (response units). To measure the equilibrium background response signal (bulk refractive index effect) control experiments were performed using a blank cell at Nef concentrations identical

to those used for specific binding studies. Equilibrium background response values (~0–20% of total response, depending on the concentration of Nef) were subtracted from the values obtained for the specific binding reactions to yield the specific response value, cRU (corrected response unit), for each concentration of Nef tested. All binding experiments were performed at 25°C with a flow rate of 10 µl/min in HBS running buffer with 1 mM DTT. The concentration range of Nef and Nef-PA1 used for binding to various GST–SH3 fusion proteins was 6–0.06 µM. After completion of an individual binding experiment the chip was washed for a further 20 min with running buffer (HBS with 1 mM DTT) at a flow rate of 15 µl/min, which was found to be sufficient to regenerate the chip. Due to the extremely high affinity interaction between biotin and streptavidin ($K_D \approx 10^{-15}$ M), this washing did not result in loss of the immobilized GST–SH3 proteins. The level of the SPR response was examined using a standard Nef solution before and after 20 programmed runs and revealed no significant change in Nef binding capacity of the chips.

Isothermal titration calorimetry

Titrations employed the OMEGA instrument (MicroCal; Wiseman *et al.*, 1989) and were performed at 25°C in 50 mM HEPES, 150 mM NaCl, 3.4 mM EDTA, 2 mM DTT, pH 7.4. Both Hck SH3 and Nef were dialyzed exhaustively, in the same container, against this buffer prior to titration. The titration was then performed as described (Lemmon and Ladbury, 1994) with 16 injections of 15 µl each of Hck SH3 (at 1.09×10^{-4} M) into a solution of Nef (1.09×10^{-5} M) in the calorimeter cell (1.39 ml). The heat of dilution of the Hck SH3 solution was determined in a separate titration of SH3 domain into buffer solution present in the cell. The heat per injection remained constant throughout this dilution and a mean value for this heat was subtracted from heats per injection measured in the binding titration. An additional control was performed for the heat of dilution of buffer into the Nef solution and this heat was also subtracted from experimental heats of dilution. In all cases the value for [sites]K_D (c value) was <100. Titration curves were fitted using ORIGIN software (MicroCal), using a non-linear least squares algorithm based on a model for a single class of binding site, as indicated by the shape of the titrations (Wiseman *et al.*, 1989). Stoichiometry, binding constant ($K_B = 1/K_D$) and ΔH were all allowed to float in the fitting procedure.

Tryptophan fluorescence spectroscopy

Fluorescence measurements were done at 18°C using a Perkin-Elmer 760-40 fluorescence spectrometer (Knudsen *et al.*, 1995). The wavelength for excitation was 290 nm and the wavelength for emission was 345 nm. Increasing amounts of 23 mM Nef PxxP peptide solution were added to 1 cm square quartz fluorescence cuvettes containing 1 ml of a 0.5 µM solution of the GST–SH3 domain fusion protein of interest in HBS buffer and the equilibrium dissociation constants (K_D values) for these interactions were determined based on the observed changes in fluorescence. Since the concentrations of SH3 domains were low, the experimental data were fitted using the following equation: $F = F_{max}\times$ [peptide]/([peptide] + K_D), where [peptide] and F are the peptide concentration and the measured protein fluorescence intensity at each point and F_{max} is the observed maximal fluorescence intensity of the protein when saturated with the peptide. Non-linear regression curve fitting using ORIGIN (MicroCal Software Inc.) was done to fit the experimental data to the above equation. In the case of Hck purified SH3 domain cleaved free of GST was also similarly tested and showed binding kinetics very similar to those observed using the GST–Hck SH3 fusion protein.

CD spectroscopy

CD measurements were done using a AVIV 62 DS CD spectrometer and data collection and processing were performed using the program provided by the manufacturer. Experiments using 50 µM protein in HBS buffer containing 1 mM DTT were carried out at three different temperatures (4, 15 and 25°C) using a 0.1 mm path length cuvette. Spectra were recorded in the wavelength range 195–240 nm with a 0.5 nm spacing and values from five individual measurements were averaged and expressed as molar mean residue ellipticity values as a function of the wavelength.

Co-precipitation assay

To examine binding of wild-type and mutant Nef proteins to different GST–SH3 fusion proteins in solution 1–4 µg (as detailed in the legend to Figure 6) of each GST–SH3 fusion protein were immobilized on glutathione–agarose beads and incubated at 4°C for 20 min with various concentrations of Nef in 20 mM HEPES, pH 7.5, 10% glycerol, 1% Triton X-100, 150 mM NaCl, 1 mM DTT (in a total volume of 1 ml). After a 20 min incubation at 4°C the beads were washed three times with the same buffer, followed by electrophoretic analysis in a 15% SDS–polyacrylamide gel. Bound Nef protein, as well as the GST–SH3 fusion protein, were visualized by Coomassie Blue staining. Peptide inhibition assays were done in an identical manner except that, in addition to Nef, a 2- to 800-fold molar excess of the peptide PVRPQVPLRPMT was also included in the binding reaction.

Acknowledgements

We thank Russ Granzow from Pharmacia Biosensor for technical advice, Julian Sturtevant at Yale University for access to the MicroCal calorimeter (supported by NIH grant GM04725), Ronan O'Brien for help with the ITC experiments, Xiaodong Wu for the Crk-SH3–C3G complex coordinates, Michael Eck for the Lck SH2-SH3 coordinates, Huguette Viguet for synthesizing oligonucleotides for these studies, Joseph Schlessinger and David Wilson for helpful discussions and David Baltimore for advice and comments on the manuscript. M.A.L. is the Marion Abbe Fellow of the Damon Runyon–Walter Winchell Cancer Research Fund (DRG-1243). This study was partially funded by NIH grant GM47021 to D.C. and a Junior Faculty Award from the Aaron Diamond Foundation for AIDS Research to K.S.

References

Alexandropoulos,K., Cheng,G. and Baltimore,D. (1995) Proline-rich sequences that bind to Src homology 3 domains with individual specificities. *Proc. Natl Acad. Sci. USA*, **92**, 3110–3114.

Brünger,A.T. (1988) *X-plor Manual*. Howard Hughes Medical Institute and Department of Molecular Biophysics and Biochemistry, Yale University, New Haven, CT.

Cheng,G., Ye,Z.S. and Baltimore,D. (1994) Binding of Bruton's tyrosine kinase to Fyn, Lyn, or Hck through a Src homology 3 domain-mediated interaction. *Proc. Natl Acad. Sci. USA*, **91**, 8152–8155.

Cicchetti,P., Mayer,B.J., Thiel,G. and Baltimore,D. (1992) Identification of a protein that binds to the SH3 region of Abl and is similar to Bcr and GAP-rho. *Science*, **257**, 803–806.

Cohen,G., Ren,R. and Baltimore,D. (1995) Modular binding domains in signal transduction proteins. *Cell*, **80**, 237–248.

Eck,M.J., Atwell,S.K., Shoelson,S.E. and Harrison,S.C. (1994) Structure of the regulatory domains of the Src-family tyrosine kinase Lck. *Nature*, **368**, 764–769.

Erpel,T., Superti-Furga,G. and Courtneidge,S.A. (1995) Mutational analysis of Src SH3 domain: the same residues of the ligand binding surface are important for intra- and intermolecular interactions. *EMBO J.*, **14**, 963–975.

Feng,S., Chen,J.K., Yu,H., Simon,J.A. and Schreiber,S.L. (1994) Two binding orientations for peptides to the Src SH3 domain: development of a general model for SH3–ligand interactions. *Science*, **266**, 1241–1247.

Huang,Y., Zhang,L. and Ho,D.D. (1995) Characterization of *nef* sequences in long-term survivors of human immunodeficiency virus type 1 infection. *J. Virol.*, **69**, 93–100.

Jones,T.A., Zou,J.Y., Cowan,S.W. and Kjeldgaarn,M. (1991) Improved methods for building protein models in electron density maps and the location of errors in these models. *Acta Crystallogr.*, **A47**, 110–119.

Kato,J.Y., Takeya,T., Grandori,C., Iba,H., Levy,J.B. and Hanafusa,H. (1986) Amino acid substitutions sufficient to convert the nontransforming p60c-src protein to a transforming protein. *Mol. Cell. Biol.*, **6**, 4155–4160.

Kawakami,T., Pennington,C.Y. and Robbins,K.C. (1986) Isolation and oncogenic potential of a novel human src-like gene. *Mol. Cell. Biol.*, **6**, 4195–201.

Knudsen,B.S., Feller,S.M. and Hanafusa,H. (1994) Four proline-rich sequences of the guanine-nucleotide exchange factor C3G bind with unique specificity to the first Src homology domain of Crk. *J. Biol. Chem.*, **269**, 32781–32787.

Knudsen,B.S., Zheng,J., Feller,S.M., Mayer,J.P., Burrell,S.K., Cowburn,D. and Hanafusa,H. (1995) Affinity and specificity requirements for the first Src homolgy 3 domain of the Crk proteins. *EMBO J.*, **14**, 2191–2198.

Kuriyan,J. and Cowburn,D. (1993) The structures of SH2 and SH3 domains. *Curr. Opin. Struct. Biol.*, **3**, 828–837.

Ladbury,J.E., Lemmon,M.A., Zhou,M., Green,J., Botfield,M.C. and Schlessinger,J. (1995) Measurement of the binding of tyrosyl phosphopeptides to SH2 domains: a reappraisal. *Proc. Natl Acad. Sci. USA*, **92**, 3199–3203.

Lemmon,M.A. and Ladbury,J.E. (1994) Thermodynamic studies of tyrosyl-phosphopeptide binding to the SH2 domain of $p56^{lck}$. *Biochemistry*, **33**, 5070–5076.

Lim,W.A., Richards,F.M. and Fox,R.O. (1994) The structural determinants of peptide binding orientation and of sequence specificity in SH3 domains. *Nature*, **372**, 375–379.

Mayer,B.J. and Baltimore,D. (1993) Signalling through SH2 and SH3 domains. *Trends Cell Biol.*, **3**, 8–13.

Murphy,S.M., Bergman,M. and Morgan,D.O. (1993) Suppression of c-Src activity by C-terminal Src kinase involves the c-Src SH2 and SH3 domains: analysis with *Saccharomyces cerevisiae*. *Mol. Cell. Biol.*, **13**, 5290–5300.

Musacchio,A., Saraste,M. and Wilmanns,M. (1994a) High-resolution crystal structures of tyrosine kinase SH3 domain complexed with proline-rich peptides. *Struct. Biol.*, **1**, 546–551.

Musacchio,A., Wilmanns,M. and Saraste,M. (1994b) Structure and function of the SH3 domain. *Prog. Biophys. Mol. Biol.*, **61**, 283–297.

Noble,M.E., Musacchio,A., Saraste,M., Courtneidge,S.A. and Wierenga,R.K. (1993) Crystal structure of the SH3 domain in human Fyn; comparison of the three-dimensional structures of SH3 domains in tyrosine kinases and spectrin. *EMBO J.*, **12**, 2617–2624.

Okada,M., Howell,B.W., Broome,M.A. and Cooper,J.A. (1993) Deletion of the SH3 domain of Src interferes with regulation by the phosphorylated carboxyl-terminal tyrosine. *J. Biol. Chem.*, **268**, 18070–18075.

O'Shannessy,D.J., Brigham,B.M., Soneson,K.K., Hensley,P. and Brooks,I. (1993) Determination of rate and equilibrium binding constants for macromolecular interactions using surface plasmon resonance: use of nonlinear least squares analysis methods. *Anal. Biochem.*, **212**, 457–468.

Pawson,T. and Schlessinger,J. (1993) SH2 and SH3 domains. *Curr. Biol.*, **3**, 434–442.

Potts,W.M., Reynolds,A.B., Lansing,T.J. and Parsons,J.T. (1988) Activation of pp60c-src transforming potential by mutations altering the structure of an amino terminal domain containing residues 90–95. *Oncogene Res.*, **3**, 343–355.

Ren,R., Mayer,B.J., Cicchetti,P. and Baltimore,D. (1993) Identification of a ten-amino acid proline-rich SH3 binding site. *Science*, **259**, 1157–1161.

Rickles,R., Botfield,M.C., Weng,Z., Taylor,J., Green,O.M., Brugge,J. and Zoller,M.J. (1994) Identification of Src, Fyn, Lyn, PI3K, and Abl SH3 domain ligands using phage display libraries. *EMBO J.*, **13**, 5598–5604.

Saksela,K., Cheng,G. and Baltimore,D. (1995) Proline-rich (PxxP) motifs in HIV-1 Nef bind to SH3 domains of a subset of Src kinases and are required for the enhanced growth of Nef^+ viruses but not for downregulation of CD4. *EMBO J.*, **14**, 484–491.

Schlessinger,J. (1994) SH2/SH3 signaling proteins. *Curr. Opin. Genet. Dev.*, **4**, 25–30.

Shugars,D.C., Smith,M.S., Glueck,D.H., Nantermet,P.V., Seillier,M.F. and Swanstrom,R. (1993) Analysis of human immunodeficiency virus type 1 *nef* gene sequences present *in vivo*. *J. Virol.*, **67**, 4639–50.

Superti Furga,G., Fumagalli,S., Koegl,M., Courtneidge,S.A. and Draetta,G. (1993) Csk inhibition of c-Src activity requires both the SH2 and SH3 domains of Src. *EMBO J.*, **12**, 2625–2634.

Terasawa,H. *et al.* (1994) Structure of the N-terminal SH3 domain of GRB2 complexed with a peptide from the guanine nucleotide releasing factor Sos. *Nature Struct. Biol.*, **1**, 891–897.

Weng,Z., Thomas,S., Rickles,R., Taylor,J., Brauer,A., Seidel-Dugan,C., Michael,W., Dreyfuss,G. and Brugge,J. (1994) Identification of Src, Fyn, and Lyn SH3-binding proteins: implications for a function of SH3 domains. *Mol. Cell. Biol.*, **14**, 4509–4521.

Wiseman,T., Williston,S., Brandts,J.F. and Lin,L.-N. (1989) Rapid measurement of binding constants and heats of binding using new titration calorimeter. *Anal. Biochem.*, **179**, 131–137.

Wittekind,M. *et al.* (1994) Orientation of peptide fragments from Sos proteins bound to the N-terminal SH3 domain of Grb2 determined by NMR spectroscopy. *Biochemistry*, **33**, 13531–13539.

Wolber,V., Rensland,H., Brandmeier,B., Sagemann,M., Hoffmann,R., Kalbitzer,H.R. and Wittinghofer,A. (1992) Expression, purification and biochemical characterisation of the human immunodeficiency virus 1 *nef* gene product. *Eur. J. Biochem.*, **205**, 1115–1121.

Wu,X., Knudsen,B., Feller,S.M., Zheng,J., Sali,A., Cowburn,D., Hanafusa,H. and Kuriyan,J. (1995) Structural basis for specific interaction of lysine-containing proline-rich peptides with the amino-terminal SH3 domain of c-Crk. *Structure*, **3**, 215–226.

Yu,H., Chen,J.K., Feng,S., Dalgarno,D.C., Brauer,A.W. and Schreiber,S.L. (1994) Structural basis for binding of proline-rich peptides to SH3 domains. *Cell*, **76**, 933–945.

Received on June 19, 1995; revised on July 19, 1995